PLASTIC HINGE ANALYSIS

By Oguzhan Bayrak[1] and Shamim A. Sheikh,[2] Members, ASCE

ABSTRACT: Predicting behavior of plastic hinges subjected to large inelastic deformations caused by extreme loads such as earthquakes plays an important role in assessing maximum stable deformation capacities of framed concrete structures. This paper presents an analytical procedure that can be used to predict the behavior of plastic hinges in reinforced concrete columns. Since the behavior of plastic hinges in concrete columns is a 3D problem, the plastic hinge analysis technique considers equilibrium, compatibility, and constitutive relations in 3D space. Complex behavioral phenomena such as softening of longitudinal bars due to inelastic buckling and reinforcing cage-concrete core interaction are incorporated in the analysis. To establish a constitutive relationship for reinforcing bars under axial compression an experimental study on 56 reinforcing bar specimens having unsupported length to bar diameter ratios ranging between 4 and 10 was conducted, and results are reported herein. Finally, the suggested analytical procedure is compared with conventional analysis techniques by predicting the sectional response of concrete column specimens. It is concluded that through the use of the analytical procedure presented here it was possible to obtain realistic estimations for the maximum deformation capacities of the plastic hinge regions of the specimens that were tested under constant axial loads and reversed cyclic displacement excursions. The concrete core-reinforcing cage interaction, which caused outward deflections in longitudinal bars, did not only reduce the ductility of longitudinal bars under compression but also reduced the maximum stress that the bars were able to achieve.

INTRODUCTION

Bayrak (1999), Bayrak and Sheikh (1998), Sheikh et al. (1994), and Sheikh and Khoury (1993) reported that in all column specimens tested during their experimental work longitudinal bar buckling was observed during the last cycles of the tests after the yielding of tie steel. Fig. 1 illustrates typical failure in the plastic hinge region of Specimen RS-12HT (Bayrak 1999). The tie spacing to longitudinal bar diameter ratio in these specimens varied from 3.5 to 7.5.

Since buckling of the longitudinal bars is generally not considered in the conventional analytical procedures to determine the response of concrete column sections, behavior at large inelastic curvatures is generally overpredicted with respect to strength and ductility Bayrak (1999). An extensive literature survey was undertaken to determine the availability of rational analytical models for the longitudinal bar buckling in tied concrete columns. Studies reported by Bresler and Gilbert (1961), Scribner (1986), Russo (1988), Papia et al. (1988), Mau and El-Mabsout (1989), and Monti and Nuti (1992) did not consider the interaction between the confined concrete core and the longitudinal bars under compression. The literature survey conducted also revealed the fact that a very limited amount of experimental data was available on reinforcing bars tested under compression. This necessitated conducting experimental research in order to establish a comprehensive database upon which a rational analytical procedure could be built.

RESEARCH SIGNIFICANCE

Determination of displacement capacity of framed concrete structures and development of design procedures based on displacement capacities of the members has been attracting considerable attention in earthquake engineering. In the overall process of predicting maximum attainable displacements and drift ratios of framed concrete structures, the behavior of plastic hinges is the most significant part of the analysis. Modeling of rather complex phenomena such as softening of longitudinal bars due to their inelastic buckling and reinforcing cage-concrete core interaction, in a rational yet simple manner, is important so that the resulting procedure can be used by practitioners. The plastic hinge analysis technique, introduced herein, is developed to address the aforementioned issues, and through its use the maximum attainable curvatures of the plastic hinges can be determined with reasonable accuracy. In addition, this analysis technique often provides improvements to the predictions of both curvature and moment quantities at large inelastic deformation levels.

Both the analytical procedure and the experimental research reported herein are aimed at predicting the response of the plastic hinges that form in reinforced concrete frames during strong ground motions. The most significant product of the suggested technique lies in its ability to offer reasonable predictions for the maximum useful deformation capacities of the reinforced concrete columns, which is otherwise very difficult if not impossible to predict through the use of the standard sectional analysis techniques.

EXPERIMENTAL PROGRAM

A total of 56 reinforcing bar specimens were tested under monotonic compression. Fig. 2 illustrates the test setup. The

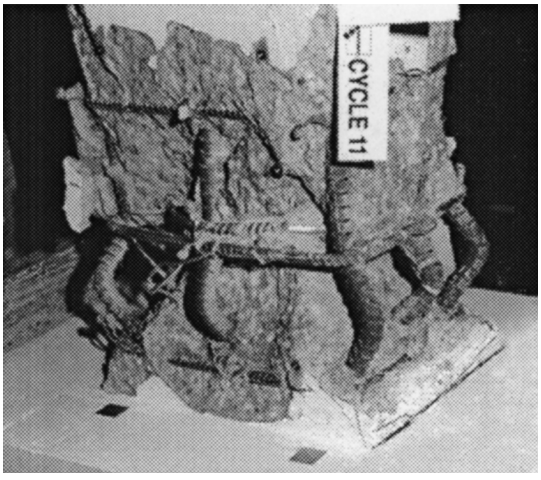

FIG. 1. Longitudinal Bar Buckling in Specimen RS-12HT

[1]Asst. Prof., Dept. of Civ. Engrg., Univ. of Texas at Austin, Austin, TX 78712.

[2]Prof., Dept. of Civ. Engrg., Univ. of Toronto, Toronto, ON, Canada.

Note. Associate Editor: John Wallace. Discussion open until February 1, 2002. To extend the closing date one month, a written request must be filed with the ASCE Manager of Journals. The manuscript for this paper was submitted for review and possible publication on January 31, 2000; revised April 27, 2001. This paper is part of the ***Journal of Structural Engineering***, Vol. 127, No. 9, September, 2001. ©ASCE, ISSN 0733-9445/01/0009-1092–1100/$8.00 + $.50 per page. Paper No. 22249.

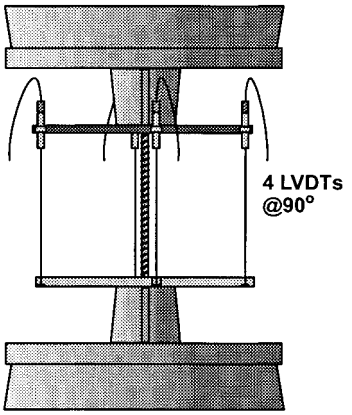

FIG. 2. Schematic of Test Setup

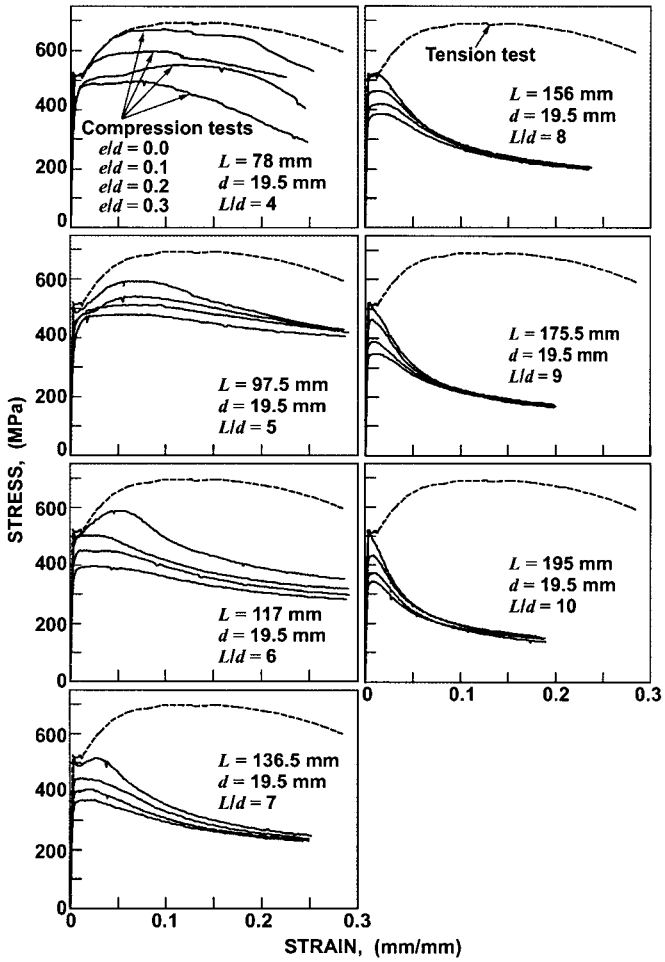

FIG. 3. Axial Stress-Strain Response of Reinforcing Bar Specimens

tensile stress-strain behavior of the Grade 400 20M bars used in this study is shown in Fig. 3. Seven different tie spacing to longitudinal bar diameter ratios (i.e., unsupported length to longitudinal bar diameter ratios) l/d were used. The smallest tie spacing to longitudinal bar diameter ratio used was 4 and the largest was 10. For each l/d ratio, four different levels of initial imperfection were tested. Initial imperfections were introduced by clamping both ends of the longitudinal bars and bending them such that the permanent midspan deflection e measured as a fraction of the longitudinal bar diameter d was equal to a predetermined value. The e/d ratios used in the experimental program ranged between 0.0 and 0.3. Table 1 illustrates the specimen details.

The alphanumeric characters in specimen designation have the following meanings. The first three characters (i.e., ''20M'') indicates that the specimens tested in this experimental program are fabricated with standard 20M-Grade 400 reinforcing bars. The fourth number illustrates the l/d ratio of the specimen. Dividing the fifth number by 10 gives the e/d ratio of a test specimen. The last number, ranging from 1 to 56, indicates the sequence of testing. For each l/d and e/d combination there are two specimens. In other words, 28 pairs of identical specimens were fabricated in order to ensure the reliability of the experimental data.

TABLE 1. Reinforcing Bar Specimens

Specimen	l (mm)	e (mm)	l/d	e/d
20M-4-0-1	78	0	4	0.0
20M-4-0-2	78	0	4	0.0
20M-4-1-3	78	2	4	0.1
20M-4-1-4	78	2	4	0.1
20M-4-2-5	78	4	4	0.2
20M-4-2-6	78	4	4	0.2
20M-4-3-7	78	6	4	0.3
20M-4-3-8	78	6	4	0.3
20M-5-0-9	97.5	0	5	0.0
20M-5-0-10	97.5	0	5	0.0
20M-5-1-11	97.5	2	5	0.1
20M-5-1-12	97.5	2	5	0.1
20M-5-2-13	97.5	4	5	0.2
20M-5-2-14	97.5	4	5	0.2
20M-5-3-15	97.5	6	5	0.3
20M-5-3-16	97.5	6	5	0.3
20M-6-0-17	117	0	6	0.0
20M-6-0-18	117	0	6	0.0
20M-6-1-19	117	2	6	0.1
20M-6-1-20	117	2	6	0.1
20M-6-2-21	117	4	6	0.2
20M-6-2-22	117	4	6	0.2
20M-6-3-23	117	6	6	0.3
20M-6-3-24	117	6	6	0.3
20M-7-0-25	136.5	0	7	0.0
20M-7-0-26	136.5	0	7	0.0
20M-7-1-27	136.5	2	7	0.1
20M-7-1-28	136.5	2	7	0.1
20M-7-2-29	136.5	4	7	0.2
20M-7-2-30	136.5	4	7	0.2
20M-7-3-31	136.5	6	7	0.3
20M-7-3-32	136.5	6	7	0.3
20M-8-0-33	156	0	8	0.0
20M-8-0-34	156	0	8	0.0
20M-8-1-35	156	2	8	0.1
20M-8-1-36	156	2	8	0.1
20M-8-2-37	156	4	8	0.2
20M-8-2-38	156	4	8	0.2
20M-8-3-39	156	6	8	0.3
20M-8-3-40	156	6	8	0.3
20M-9-0-41	175.5	0	9	0.0
20M-9-0-42	175.5	0	9	0.0
20M-9-1-43	175.5	2	9	0.1
20M-9-1-44	175.5	2	9	0.1
20M-9-2-45	175.5	4	9	0.2
20M-9-2-46	175.5	4	9	0.2
20M-9-3-47	175.5	6	9	0.3
20M-9-3-48	175.5	6	9	0.3
20M-10-0-49	195	0	10	0.0
20M-10-0-50	195	0	10	0.0
20M-10-1-51	195	2	10	0.1
20M-10-1-52	195	2	10	0.1
20M-10-2-53	195	4	10	0.2
20M-10-2-54	195	4	10	0.2
20M-10-3-55	195	6	10	0.3
20M-10-3-56	195	6	10	0.3

Note: d = 19.5 mm.

INSTRUMENTATION AND TESTING

The specimens were not instrumented by strain gauges due to the following reasons:

- Installation of strain gauges would disturb the geometry of the deformed bars and cause a decrease in the cross-sectional area.
- Strain gauges would give the local strains measured over a gauge length of 5 mm or so. This strain has no actual physical meaning after the initiation of longitudinal bar buckling in a column test. Once buckling initiates in a column, the reinforcing bar strains would be different than the concrete core strains at that section. Therefore, from a theoretical perspective these strains would not correspond to the longitudinal strains calculated at the extreme compression fiber of the core as calculated in a standard sectional analysis. What is more important is the average strain calculated between the two supports simulating the two tie sets that anchor the longitudinal bar to the concrete core. This average tie strain is assumed to correspond to the average core concrete strain measured between the two tie sets by means of LVDTs.

As a result four LVDTs having gauge lengths equal to the unsupported bar lengths are used to calculate average axial deformations and axial strains (Fig. 2). The 1,000-kN MTS testing machine housed in the Structural Testing Laboratories of the University of Toronto was used under displacement control to test all the specimens.

TEST RESULTS

Responses of the specimens are represented graphically in the form of axial stress versus axial strain relationships. As mentioned earlier for each l/d and e/d combination, two specimens were tested to ensure reliability of the test data. Each curve presented in Fig. 3 is obtained by averaging the two curves along the stress axis. In most cases responses obtained from the two specimens with the same l/d and e/d values are almost identical, with the maximum stress difference being <2%.

For a give l/d ratio, an increase in the e/d ratio causes reductions in strength and ductility. Similarly, for a given e/d ratio, an increase in the l/d ratio reduces the strength and ductility of the reinforcing bars under compression. For initially straight bars, there is a critical l/d ratio, equal to 7, beyond which the postbuckling load-carrying capacity is smaller than the yield load. Based on the finite-element analysis results, Mau and El-Mabsout (1989) reported this value to be equal to 8. For $l/d = 7$, Mau and El-Mabsout (1989) predicted the postbuckling stress to be 9% larger than the yield stress. Mander et al. (1988) reported that an l/d ratio of 6 can be used as a design limit. Mau and El-Mabsout (1990) reported that for l/d ratios smaller than or equal to 6, stress-strain behavior of reinforcing bars under tension and compression are practically the same. Curves illustrated in Fig. 4 are in reasonably good agreement with this observation. However, it should be appreciated that the reinforcing cage-concrete core interaction is neglected while drawing these general conclusions.

The concrete core under axial compression has the tendency to expand laterally, bear against the longitudinal bars, and introduce transverse loads on axially compressed longitudinal bars. This effect is considered in the plastic hinge analysis presented here. The following observations can be made based on the experimental data presented in Fig. 3:

- It can be observed in Fig. 3 that the concrete core-reinforcing cage interaction, which would cause an outward deflection of longitudinal bars, would not only reduce the ductility of longitudinal bars under compression but also reduce the attainable maximum strength.
- For l/d ratios under 6, the yield strength of longitudinal bars can be achieved up to $e/d = 0.1$. For columns with high curvature ductility demand, the tie spacing to longitudinal bar diameter ratio should be kept under 6.
- A yield plateau is observed in all longitudinal bars having l/d ratios up to 8 for all e/d ratios. The postbuckling strengths of reinforcing bars with l/d ratios <8 and $e/d = 0$ are equal to or larger than the yield strength. For columns with moderate curvature ductility demands, l/d ratios up to 8 can be used.
- For cases where longitudinal bars are expected to deform inelastically under compressive stresses without losing any strength, tie spacing to longitudinal bar diameter ratios >8 should be avoided. Such large tie spacings are only satisfactory in cases where ductile sectional performances are not expected.

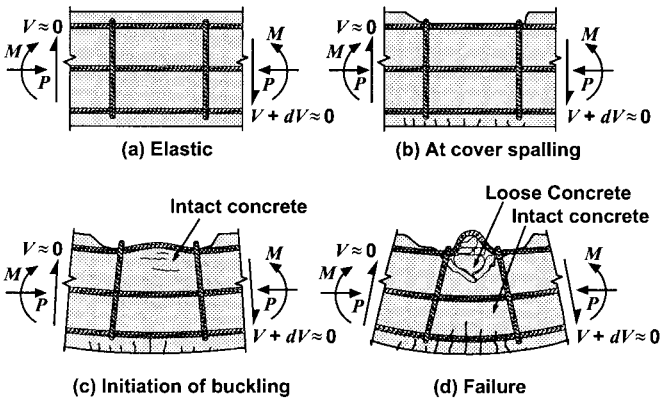

FIG. 4. Plastic Hinge under Axial Compression and Bending

PLASTIC HINGE ANALYSIS

Conventional plastic hinge analysis of a reinforced concrete section is performed using a sectional analysis program in which effects of confinement are considered. Reinforcing bars are generally assumed to display identical behavior under tension and compression. As the name ''sectional analysis'' implies, the most critical section in the plastic hinge region is analyzed. Observations during the column tests (Sheikh and Khoury 1993; Sheikh et al. 1994; Bayrak and Sheikh 1998; Bayrak 1999) indicated that longitudinal bars displayed buckling in almost all the columns before their failure. After a certain point in the test, the local longitudinal bar strains at a section measured by strain gauges started to differ from those obtained by drawing the strain profile based on the ''plane sections remain plane'' assumption of the beam bending theory. This phenomenon indicates the initiation of buckling of the longitudinal bars (Bayrak and Sheikh 1998).

The conventional sectional analysis up to the initiation of longitudinal bar buckling is quite valid, but beyond this point the response of a section can be predicted with reasonable accuracy only if the behavior of the longitudinal bars is determined by considering the phenomenon of buckling. This would mean that the longitudinal bar strains would be locally different than the concrete core strains. However, the total compressive deformation between the two tie sets located at either side of the critical section is identical for both the concrete core and the longitudinal bars. In other words, it is assumed that the integrity of the bond between the concrete core and the longitudinal bars exists only at the sections where ties are present. Fig. 4 illustrates this assumption, and Fig. 1 shows the experimental evidence that supports the same argument. The plastic hinge analysis procedure uses this displacement compatibility requirement along with equilibrium considerations and constitutive relations to evaluate the plastic hinge response of tied columns. The following is a step-by-step de-

TABLE 2. Concrete Strains at Cover Spalling and Initiation of Longitudinal Bar Buckling

Specimen	f'_c (MPa)	$\varepsilon_{spalling}$ (mm/mm)	$\varepsilon_{buckling}$[a] (mm/mm)
ES-1HT	72.1	0.0026	0.008
AS-2HT	71.7	0.0024	0.012
AS-3HT	7.18	0.0022	0.011
AS-4HT	71.9	0.0023	0.012
AS-5HT	101.8	0.0029	0.010
AS-6HT	101.9	0.0027	0.012
AS-7HT	102.0	0.0030	0.009
ES-8HT	102.2	0.0029	0.008
RS-9HT	71.2	0.0027	0.011
RS-10HT	71.1	0.0026	0.012
RS-11HT	70.8	0.0025	0.011
RS-12HT	70.8	0.0028	0.009
RS-13HT	112.1	0.0032	0.013
RS-14HT	112.1	0.0031	0.014
RS-15HT	56.2	0.0025	0.015
RS-16HT	56.2	0.0027	0.012
RS-17HT	74.1	0.0025	0.013
RS-18HT	74.1	0.0026	0.012
RS-19HT	74.2	0.0024	0.014
RS-20HT	74.2	0.0027	0.011
WRS-21HT	91.3	0.0029	0.014
WRS-22HT	91.3	0.0028	0.015
WRS-23HT	72.2	0.0025	0.013
WRS-24HT	72.1	0.0026	0.013

[a]Initiation of buckling is determined by visual inspection during the test.

scription of the procedure followed for the analysis of plastic hinges.

1. Standard sectional analysis procedure is followed before the initiation of buckling of the longitudinal bars.
2. At the initiation of bar buckling, the axial strain is determined using the experimental evidences, such as those listed in Table 2 (Bayrak 1999).
3. At this point the concrete cover has already spalled off and severe internal microcracking at the concrete core has taken place. To determine tie stress, a relationship that provides average tie strains for a given axial compressive strain is needed. To establish this relationship, experimental data from concentric axial compression tests of tied columns [e.g., Sheikh (1978)] were used.
4. The tie forces are mainly generated as a result of core concrete bearing against the reinforcing bars. Therefore, the total magnitude of the transverse forces acting on longitudinal bars can be determined using equilibrium equations.
5. By using proper boundary conditions and an assumed shape function for the forces acting on longitudinal bars, their outward deflection at the midheight between two sets of ties can be calculated. Dividing this deflection by the longitudinal bar diameter would yield an e/d ratio used in the tests described in the earlier sections.
6. Using the e/d ratio calculated above and the l/d ratio, the relevant stress-strain curve for reinforcing bars under compression can be selected and used as the constitutive relationship for compressed bars in the sectional analysis.

In the suggested analysis procedure, the following four constitutive relations are used after the initiation of longitudinal bar buckling.

- Stress-strain relationship for unconfined cover concrete
- Stress-strain relationship for confined core concrete
- Stress-strain relationship for longitudinal bars under tension
- Stress-strain relationship for longitudinal bars with initial imperfections under compression

In the following sections, derivation of the constitutive relations needed for the plastic hinge analysis is described.

Confined Concrete Expansion Ratio

A relationship that provides average tie strains for a given axial compressive strain is needed to perform the plastic hinge analysis procedure described above. The confined concrete expansion ratio β_{exp} can be defined as the ratio of transverse strain to axial strain

$$\beta_{exp} = \frac{\varepsilon_{transverse}}{\varepsilon_{axial}} \quad (1)$$

Experimental data from well-instrumented tied columns tested under monotonic concentric axial compression was used to establish this relationship (Sheikh 1978). Twenty-four square columns were tested under increasing concentric axial compression to failure in the test program. All the columns were 305 mm (12 in.) square and 1,960 mm (77 in.) long. To prevent failure in the end zones, sections were gradually enlarged to 305 × 508 mm (12 × 20 in.). The volumetric ratio of lateral reinforcement to core concrete ranged between 0.76 and 2.39%, and the longitudinal reinforcement content varied from 1.72 to 3.67% of the gross cross-sectional area. Concrete strength ranged between 30 and 40 MPa. Longitudinal reinforcement distribution and the lateral reinforcement configuration were considered as variables influencing the area of effectively confined concrete in the core. An analytical model to predict the confined concrete stress-strain relationship was also developed by Sheikh and Uzumeri (1982).

Tie strains were measured at each load increment along with the axial strains. Several strain gauges attached to two tie sets located at the midheight of the column were used to determine the tie strains. Tie strains were also measured by means of

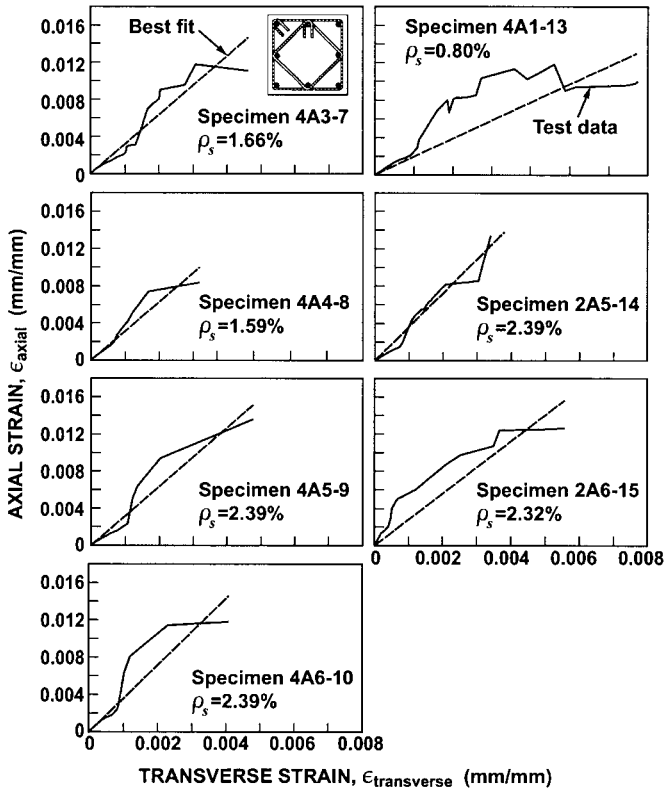

FIG. 5. Transverse Strain-Axial Strain Response of Specimens

LVDTs directly attached to the ties. Axial strains were determined as an average of the four vertical LVDTs attached to threaded rods that extended out of the concrete core. Detailed information about this experimental work is available elsewhere (Sheikh 1978; Sheikh and Uzumeri 1982). All columns with A-type reinforcement configuration (Fig. 5) from the experimental data of Sheikh (1978) are analyzed here in order to evaluate the corresponding confined concrete expansion ratio β_{exp}. It is believed that different reinforcement configurations would yield different confined concrete expansion ratios. Table 3 illustrates the details of the columns having A-type reinforcement configuration.

Linear best-fit curves are plotted with the experimental data in Fig. 5. It is appreciated that this is a simple approach in terms of relating axial strains to transverse strains. The behavior may be modeled more accurately with a piecewise linear or higher-order fit. The slope of the line would be constant up to the spalling of cover concrete. After this point, there would be a change in slope, and axial strains would increase more rapidly. Then, yielding of longitudinal bars would occur that would increase the axial strain rate. Finally, when the transverse ties yield, the slope of the curve would change again. Strain hardening of longitudinal bars and transverse ties would further complicate the problem. The strains at which cover spalling, longitudinal bar yielding, and transverse reinforcement yielding occur would vary with the varying materials' properties. An accurate evaluation of this would require an extensive experimental study. The error introduced in the analytical procedure by assuming a straight-line fit is recognized but is considered to be acceptable for this study.

The confined concrete expansion ratios for the eight specimens are the slopes of the straight-line curve fits shown on Fig. 5. Table 4 shows the confined concrete expansion ratios β_{exp} calculated for the A-type columns along with the maximum axial and transverse strains. These strains are not necessarily the maximum attainable strains. They are the maximum reliable strains recorded during testing before the saturation of the strain gauge readings. It was observed that the confined concrete expansion ratios decrease with the increasing volumetric ratio of tie steel to concrete core ρ_s. Specimen 2A1-1 is the only exception to this statement. A close examination of the test data indicates that the instrumented ties

TABLE 3. Details of Specimens with A-Type Reinforcement Configuration (Sheikh 1978)

		Lateral Reinforcement				Longitudinal Reinforcement		
Specimen	f'_c (MPa)	Size (mm)	Spacing (mm)	ρ_s (%)	f_{yh} (MPa)	Number and size (#)	ρ_l (%)	f_{yl} (MPa)
2A1-1	37.5	4.6	55	0.80	508	8-#5	1.72	373
4A3-7	40.9	7.7	74	1.66	514	8-#7	3.33	386
4A4-8	40.9	4.6	29	1.59	532	8-#7	3.33	386
4A5-9	40.5	9.2	74	2.39	496	8-#7	3.33	386
4A6-10	40.7	6.1	34	2.32	498	8-#7	3.33	386
4A1-13	31.3	4.6	55	0.80	518	8-#7	3.33	438
2A5-14	31.5	9.2	74	2.39	482	8-#5	1.72	404
2A6-15	31.7	6.1	34	2.32	498	8-#15	1.72	404

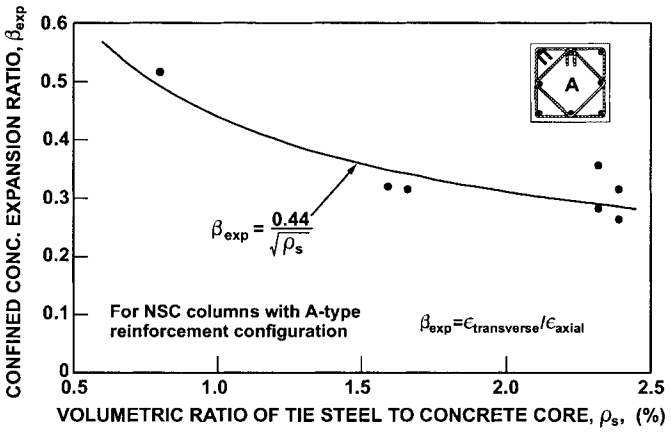

FIG. 6. Confined Concrete Expansion Ratio for A-Type NSC Columns

of Specimen 2A1-1 were not the most critical ties in this column. The measured tie strains do not represent the largest tie strains reached in that experiment. This data point was, therefore, ignored in the regression analysis performed to evaluate the relationship between the volumetric ratio of tie steel to concrete core ρ_s and the confined concrete expansion ratio β_{exp}. Fig. 6 illustrates the results of the regression analysis.

The relationship derived with the regression analysis [(2)] is only applicable for normal strength concrete (NSC) columns having A-type reinforcement configuration. Different reinforcement configurations, lateral steel strength and higher concrete strength may result in a different relationship

$$\beta_{exp} = \frac{\varepsilon_{transverse}}{\varepsilon_{axial}} = \frac{0.44}{\sqrt{\rho_s}} \tag{2}$$

where ρ_s = volumetric ratio of tie steel to concrete core, expressed as a percent.

MECHANICS OF LONGITUDINAL BAR BUCKLING IN TIED COLUMNS

The reinforcing cage-core concrete interaction problem is studied in this section. If the axial strain at which the longitudinal bar buckling initiates is known the corresponding tie strain can be determined from (2). Fig. 7 illustrates the 3D free-body diagram of a longitudinal bar in a plastic hinge region.

A simplified 2D model is also shown in Fig. 7 in which the longitudinal bar is subjected to a sinusoidal force function. At sections where there are lateral restraints caused by tie corners the force is higher. At the midheight between two tie sets, the force is smaller as the longitudinal bar can deflect outward and the core can expand with lesser restraint. Eq. (3) gives the variable forcing function used in this study and is also shown in Fig. 7

$$F(x) = F_o + F_v \cdot \cos\left(\frac{2\pi x}{s}\right) \geq 0 \tag{3}$$

where F_o = average force acting on the longitudinal bar; F_v = magnitude of the variable part of the forcing function; x =

TABLE 4. Confined Concrete Expansion Ratios β_{exp}

	Specimen							
Parameter	2A1-1	4A3-7	4A4-8	4A5-9	4A6-10	4A1-13	2A5-14	2A6-15
β_{exp}	0.21	0.32	0.32	0.32	0.28	0.52	0.26	0.36
ρ_s (%)	0.80	1.66	1.59	2.39	2.39	0.80	2.39	2.32
max($\varepsilon_{transverse}$) millistrain	2.19	4.63	3.20	4.77	4.09	6.73	3.40	5.67
max(ε_{axial}) millistrain	8.68	11.81	8.40	13.61	11.80	11.81	13.40	12.61

coordinate measured along the length of a longitudinal bar; and s = tie spacing.

The variables F_o and F_v are the two unknowns that can be determined by using force and geometric boundary conditions. The force boundary condition or the static equilibrium requirement is given by (4).

$$F_{\text{tie}} = 2 \cdot \int_0^{s/2} F(x)\, dx \tag{4}$$

For a corner longitudinal bar in a tied column with A-type reinforcement configuration, the total tie force F_{tie} can be expressed as follows:

if $\varepsilon_{\text{transverse}} \leq \varepsilon_y$

$$F_{\text{tie}} = 2 \cdot A_{1\,\text{tie}} \cdot \sin\left(\frac{\pi}{4}\right) \cdot E_{\text{tie}} \cdot \varepsilon_{\text{transverse}} \tag{5}$$

if $\varepsilon_{\text{transverse}} > \varepsilon_y$

$$F_{\text{tie}} = 2 \cdot A_{1\,\text{tie}} \cdot \sin\left(\frac{\pi}{4}\right) \cdot f_y \tag{6}$$

where $A_{1\,\text{tie}}$ = cross-sectional area of one tie leg; and E_{tie} = modulus of elasticity of the tie steel.

The probable buckling directions of all the longitudinal bars in a tied column with A-type reinforcement configuration is also shown in Fig. 7. Expressions similar to (5) and (6) can be derived for any of the longitudinal bars shown in this figure.

The geometric boundary condition used in determining the two unknown quantities in (3) is described in (7). The derivation of this equation is based on the premise that, when the tie spacing is equal to the critical tie spacing, the minimum value of the forcing function should be equal to zero. In other words, for the tie spacing $s = s_{cr}$; at $x = s_{cr}/2$, $F(x)$ should be equal to zero. In other words, the critical tie spacing can be defined as the tie spacing that generates zero confining pressure at the midsection between the two tie sets (i.e., when the effectively confined concrete area is equal to zero at this section)

$$F_v = F_o \cdot \left(\frac{s}{s_{cr}}\right)^2 \tag{7}$$

where s_{cr} = critical tie spacing that would yield to an effectively confined concrete area of zero at the midheight in between two adjacent sets of ties. With 45° compression cones, assumption $s_{cr} = h_c/2$ (where h_c = dimension of confined concrete core measured from center to center of the perimeters ties) (Sheikh 1978). Other assumptions may also be used in determining s_{cr}.

The following limit condition can be verified using (7). If $s = 0$, F_v is equal to zero. This would mean that the force applied to the longitudinal bars would be constant. In other words, if the longitudinal bars are supported by a thin shell ($s = 0$), there would be a uniform transverse force acting on them. With substitution from (7), (3) can be written

$$F(x) = F_o \cdot \left[1 + \left(\frac{s}{s_{cr}}\right)^2 \cdot \cos\left(\frac{2\pi x}{s}\right)\right] \tag{8}$$

Having determined the forcing function [(8)], the deflection of the midsection of the longitudinal bar relative to the deflection at tie levels can be calculated using the beam flexure theories. Any structural analysis technique can be used to calculate this deflection. However, it must be recognized that the bending moments created in the longitudinal bar under consideration may reach the elastic limit resulting in the formation of plastic hinges in the bar at tie levels. Depending on the sophistication level needed, the effects of the axial stress on the longitudinal bars to the outward deflection (i.e., the second order effects) may be included in the analysis. However, at this stage of the analysis, it is believed that this level of sophistication is not needed and hence is not considered in the current study. Fig. 8 illustrates an infinitesimal element in a longitudinal bar.

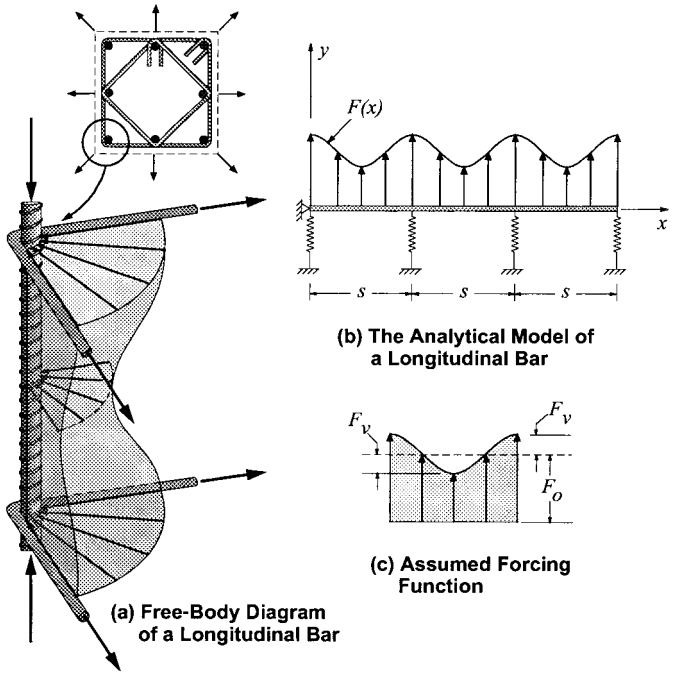

FIG. 7. Longitudinal Bar Model and Assumed Forcing Function

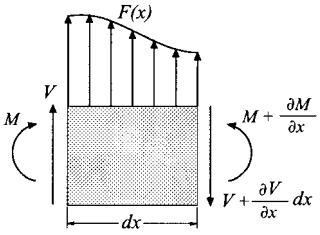

FIG. 8. Infinitesimal Element in Longitudinal Bar

The moment equilibrium equation can be obtained by summing moments about the centroidal axis at the right-hand face of the segment as follows:

$$M + V \cdot dx - \left(M + \frac{\partial M}{\partial x}\, dx\right) = 0 \tag{9}$$

Eq. (9) can be simplified further to obtain the standard static relationship between shear and moment [(10)].

$$\frac{\partial M}{\partial x} = V \tag{10}$$

Introducing the moment-curvature relationship, the relationship between the shear force and the applied transverse forcing function, (11) can be obtained for transverse deflection v

$$\frac{\partial^2}{\partial x^2}\left(EI\,\frac{\partial^2 v}{\partial x^2}\right) = F_o \cdot \left[1 + \left(\frac{s}{s_{cr}}\right)^2 \cdot \cos\left(\frac{2\pi x}{s}\right)\right] \tag{11}$$

The solution of (11) shown above yields the expression that can be used to calculate the transverse deformations of a longitudinal bar. Eq. (12) illustrates this expression

TABLE 5. Summary of Deflection Calculations

Case	Tie size (#)	Longitudinal bar size (#)	Tie spacing (mm)	f_{yl} (MPa)	f_{yt} (MPa)	E (MPa)	F_o (N/mm)	F_v (N/mm)	Δ_{mid} (mm)
1	10M	20M	150	400	400	200,000	377	94	0.8
2	10M	20M	200	400	400	200,000	283	126	2.4
3	10M	20M	300	400	400	200,000	189	189	12

$$v(x) = \frac{1}{EI}\left[F_o\left(\frac{x^4}{24} + \left(\frac{s}{s_{cr}}\right)^2 \cdot \left(\frac{s}{2\pi}\right)^4 \cdot \cos\left(\frac{2\pi x}{s}\right)\right) + c_1\frac{x^3}{6} + c_2\frac{x^2}{2} + c_3 x + c_4\right] \quad (12)$$

where E = modulus of elasticity of longitudinal bars; I = moment of inertia of the longitudinal bars; and c_i = integration constants to be determined using the geometric and force boundary conditions, where i = 1, 2, 3, 4.

In determining the integration constants, c_1, c_2, c_3, and c_4, the maximum negative and positive moments must be compared with the elastic limits, and if there is any plastification, plastic hinges should be introduced. Bearing these in mind, the deflection and slope of the bar at $x = 0$ and $x = s$ are set to be equal to zero, and hence the integration constants are evaluated. Eq. (12) is further simplified by substituting the integration constants back into the original equation. As a result, maximum deflection Δ_{mid} at midspan ($x = s/2$) of a longitudinal bar can be calculated using (13) if there is no plastification along the length of the bar

$$\Delta_{mid} = \frac{F_o}{EI}\left[\frac{s^4}{384} - \left(\frac{s}{s_{cr}}\right)^2 \cdot \left(\frac{s^4}{8\pi^4}\right)\right] \quad (13)$$

In cases where there are plastic hinge formations at the tie set levels, the midspan deflection can be calculated using (14). To obtain this equation, the deflections of the bar at $x = 0$ and $x = s$ are set to be equal to zero, and moments at these locations are set to be equal to plastic moment capacity of the longitudinal bar. Four integration constants are hence determined and substituted back into (12)

$$\Delta_{mid} = \frac{F_o}{EI}\left[\frac{5s^4}{384} + \left(\frac{s}{s_{cr}}\right)^2 \cdot \left(\frac{s^4(\pi^2 - 4)}{32\pi^4} - \frac{s^4}{8\pi^4}\right)\right] - \left(\frac{f_{yl}}{EI}\right)\left(\frac{r^3 \cdot s^2}{6}\right) \quad (14)$$

where f_{yl} = yield stress of longitudinal bars; and r = radius of longitudinal bars.

The concepts described above and the relative magnitude of the quantities can be better appreciated through a numerical example. Table 5 summarizes the deflection calculations performed on a column where the critical tie spacing is taken as 300 mm. Three different tie spacings are used to calculate the midspan deflections. For the first case, the tie spacing is assumed to be equal to half of the critical tie spacing; for the second case, tie spacing is taken as 2/3 of the critical tie spacing; and for the third case, the tie spacing is equal to the critical tie spacing. The tie strain in all three cases is assumed to be larger than or equal to the yield strain. This is a practical and fairly accurate assumption, because yielding of transverse ties had been observed before any noticeable deflection of longitudinal bars in all 24 well-confined column tests carried out by Bayrak (1999), as discussed in the previous chapters.

It must be noted that for all three cases, plastification in the longitudinal bars at the level of ties is predicted, and therefore (14) is used for deflection calculations. For the third case, where the tie spacing is kept equal to the critical tie spacing, the midspan deflection is 12 mm. Reducing the tie spacing to 2/3 of the critical tie spacing reduces this deflection to 2.4 mm. Further reduction of tie spacing to $0.5s_{cr}$ reduces the midspan deflection down to 0.8 mm. Reduction of the tie spacing for a given critical spacing, which is a function of the size of the concrete core, results in a decrease of the e/d ratio, a parameter previously described and hence improves the behavior of longitudinal bars under compression as clearly shown in Fig. 3.

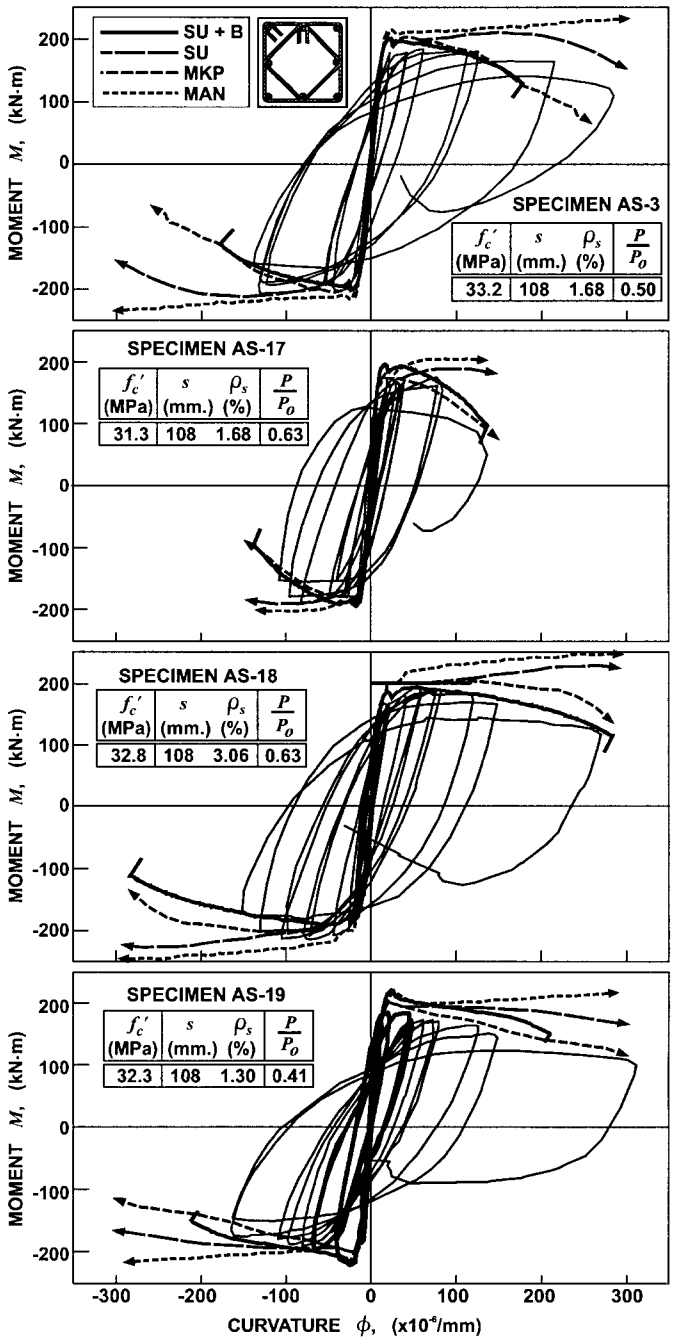

FIG. 9. Experimental and Predicted Moment-Curvature Behavior of Specimens

All the tools needed for various steps described earlier are available at this point. Therefore, the response of a section located in the plastic hinge region of a concrete column can be predicted using the plastic hinge analysis procedure. At this point it should be appreciated that the equations presented herein are derived for cases where buckling over one tie spacing takes place. For cases where one or two tie sets rupture the existence of ruptured tie sets can be ignored, and spacing can be modified accordingly so that the equations presented herein can be used. In reality, according to the principal of minimum potential energy, the mechanism that would require minimum energy to be stored in the system is the governing mechanism of failure and hence that mechanism must be used in the analysis.

The stress-strain behavior of reinforcing bars under compression will vary with varying material properties as determined by a tension test. It is believed that f_u/f_y, $\varepsilon_u/\varepsilon_y$, presence of a yield plateau, e/d, and l/d are the parameters that would influence the behavior of reinforcing bars under compression. In the current study, Grade 400 20M bars were tested under monotonic compression, the effects of e/d and l/d on the compressive behavior of reinforcing bars were studied.

APPLICATIONS OF PLASTIC HINGE ANALYSIS

Application to the plastic hinge analysis to predict the experimental behavior of column specimens is summarized in this section. Fig. 9 illustrates the sectional response of four A-type Specimens AS-3, AS-17, AS-18, and AS-19 tested by Sheikh and Khoury (1993). Table 6 illustrates the details of these test specimens.

The moment-curvature predictions, obtained using the confined concrete stress-strain relationships suggested by Sheikh and Uzumeri (1982) (SU), Kent and Park (1971) (MKP), and Mander (1988) (MAN), are also shown in Fig. 9. In the conventional sectional analyses performed to obtain the sectional responses, the aforementioned confined concrete stress-strain relationships are used for the core concrete. An unconfined concrete stress-strain relationship is used for the cover concrete and stress-strain relationships obtained from tensile coupon tests is used for longitudinal bars under tension and compression. Predictions obtained using the plastic hinge analysis procedure, with Sheikh and Uzumeri model (SU + B), are also shown in Fig. 9. The computer program, SecRes99 (Bayrak 1999), was used to obtain the predictions shown in Fig. 9. The following conclusions can be drawn about the predictions obtained.

Sheikh and Uzumeri (1982) and Mander (1988) models have the tendency to overpredict the section's moment capacity at large curvatures. The overpredictions provided by the model of Mander (1988) are considerably higher than those provided by the model of Sheikh and Uzumeri (1982). The use of the confined concrete stress-strain relationship suggested by Kent and Park (1971), on the other hand, results in underestimation of moment capacities at large deformations in some cases.

The use of the plastic hinge analysis procedure resulted in reasonably accurate predictions for the behavior of sections located in the plastic hinge region of the test specimens. The confined concrete model from Sheikh and Uzumeri (1982) was employed in this analysis. The stress-strain behavior of unconfined concrete was obtained from standard cylinder tests. Coupon tests were used for tensile stress-strain characteristics of steel. The response of longitudinal reinforcing bars under compression, shown in Fig. 3, was used in the analysis. The axial strains and transverse tie strains are related by using the confined concrete expansion ratio, introduced herein.

Conventional sectional analyses, using any of the aforementioned confined concrete stress-strain relationships, could not provide a prediction for the ultimate curvature that can be attained. With the use of the plastic hinge analysis technique presented here, the reduction in the load-carrying capacity of longitudinal bars, as a result of their buckling, can be predicted. The ultimate curvature and hence the failure of a column can therefore be determined with reasonable accuracy.

The procedure to analyze plastic hinge regions was checked for NSC columns tested by Sheikh and Khoury (1993), because the confined concrete expansion ratio β_{exp} could only be developed for NSC based on the available experimental data.

Azizinamini and Kuska (1994) conducted an experimental program on nine 2/3-scale columns with cross sections of 305 $\times$ 305 mm. Four of the columns tested were made with NSC. Details of these columns are included in Table 7, and further information on this experimental work is available elsewhere (Azizinamini and Kuska 1994). All test specimens were tested under low axial load levels. The maximum tip displacements of four NSC specimens were calculated using the plastic hinge analysis technique and integrating curvatures over the length of the test specimens. Table 7 includes both the experimental and the predicted maximum attainable tip displacements of these columns. The ratios of the predicted maximum tip displacements to maximum tip displacements recorded during the experiments are 0.88, 1.14, 1.03, and 1.15 for the test specimens. The use of the plastic hinge analysis technique resulted

TABLE 6. Details of Column-Stub Specimens

		Lateral Reinforcement					Longitudinal Reinforcement			Axial Load	
Specimen	f'_c (MPa)	Size (#)	Spacing (mm)	ρ_s (%)	f_{yh} (MPa)	$\frac{A_{sh}}{A_{sh(ACI)}}$	Number and size (#)	ρ_t (%)	f_{yl} (MPa)	$\frac{P}{f'_c A_g}$	$\frac{P}{P_o}$
AS-3	33.2	#3	108	1.68	507.4	1.43	8-#6	2.44	508.1	0.60	0.50
AS-17	31.3	#3	108	1.68	507.4	1.52	8-#6	2.44	508.1	0.77	0.63
AS-18	32.8	#4	108	306	464.0	2.41	8-#6	2.44	508.1	0.77	0.63
AS-19	32.3	#3 and 6 mm	108	1.30	507.4, 461.9	1.12	8-#6	2.44	508.1	0.47	0.40

TABLE 7. NSC Column Specimens Tested by Azizinamini and Kuska (1994)

		Lateral Reinforcement			Longitudinal reinforcement, number and size		Maximum Tip Displacement	
Specimen	f'_c (MPa)	Size (#)	Spacing (mm)	$\frac{A_{sh}}{A_{sh(ACI)}}$	(#)	Axial load	Experimental (mm)	Predicted (mm)
D60-7-4-2 5/8-0.2P	53.8	4	67	1.42	8-#6	$0.2P_o$	99	87
D60-7-3C-1 5/8-0.2P	50.9	3	41	1.50	8-#6	$0.2P_o$	130	148
D60-4-3C-2 5/8-0.2P	26.3	3	67	1.80	8-#6	$0.2P_o$	29	30
D60-4-3C-2 5/8-0.4P	27.0	3	67	1.80	8-#6	$0.4P_o$	20	23

in reasonably good predictions for the maximum displacements of the NSC columns tested by Azizinamini and Kuska (1994).

CONCLUSIONS

The following conclusions can be drawn based on the study reported here:

- The concrete core-reinforcing cage interaction, that would cause an outward deflection of longitudinal bars not only reduced the ductility of longitudinal bars under compression but also reduced the attainable maximum stress.
- Three analytical models used in the study provided reasonable estimates for the sectional behavior of NSC columns tested by Sheikh and Khoury (1993). Models of Sheikh and Uzumeri (1982) and Mander (1988) had the tendency to overestimate section's moment capacity at large curvatures. The overestimation provided by the model of Mander (1988) is generally higher than those provided by the model of Sheikh and Uzumeri (1982). Overestimation of the response can be attributed to the overestimation of the contribution of longitudinal bars in compression.
- Conventional sectional analyses are terminated artificially as the curvature values get very large and therefore are incapable of predicting the ultimate curvatures that can be attained. This artificial interference was not needed when the plastic hinge analysis was used.
- The use of the plastic hinge analysis procedure along with the model of Sheikh and Uzumeri (1982) resulted in accurate predictions for the behavior of sections located in the plastic hinge regions of the test specimens. For the analyses performed to predict sectional behavior of the specimens tested by Sheikh and Khoury (1993), the load-carrying capacity of the longitudinal bars diminished with increasing curvatures and sectional equilibrium could not be attained after a certain curvature.
- For high curvature ductility demands the tie spacing l to longitudinal bar diameter d ratio should be kept under 6. For l/d ratios under 6, the yield strength of longitudinal bars can be achieved up to $e/d = 0.1$, where e is the initial midheight deflection. In other words, the presence of initial imperfections or outward deflections introduced by the expanding core concrete are not likely to have severe adverse effects on the performance of the longitudinal bars for l/d ratios under 6.
- For moderate curvature ductility demands, the l/d ratio should be kept under 8. It must be noted that a yield plateau is observed in all 20M longitudinal bars having l/d ratios up to 8. Similarly, the postbuckling strengths of reinforcing bars with l/d ratios <8 and $e/d = 0$ are equal to or larger than the yield strength. For cases where longitudinal bars are expected to deform inelastically under compressive stresses without losing any strength, tie spacing to longitudinal bar diameter ratios greater than or equal to 9 should be avoided. Such large tie spacings are only satisfactory in cases where ductile sectional performances are not needed.

ACKNOWLEDGMENTS

Research reported here was supported by grants from the Natural Sciences and Engineering Council of Canada. The experimental work was performed in the Structural Testing Laboratories of the University of Toronto.

REFERENCES

Azizinamini, A., and Kuska, S. (1994). ''Seismic behavior of high-strength concrete columns.'' *Proc., 5th U.S. Nat. Conf. on Earthquake Engineering*, Vol. 2, 599–608.

Bayrak, O. (1999). ''Seismic performance of rectilinearly confined high strength concrete columns.'' PhD thesis, University of Toronto, Toronto.

Bayrak, O., and Sheikh, S. A. (1988). ''Confinement reinforcement design considerations for ductile HSC columns.'' *J. Struct. Engrg.*, ASCE, 124(9), 999–1010.

Bresler, B., and Gilberg, P. H. (1961). ''Tie requirements for reinforced concrete columns.'' *ACI J.*, 58(5), 555–570.

Kent, D. C., and Park, R. (1971). ''Flexural members with confined concrete.'' *J. Struct. Div.*, ASCE, 97(7), 1969–1990.

Mander, J. B., Priestley, M. J. N., and Park, R. (1988a). ''Theoretical stress-strain model for confined concrete.'' *J. Struct. Engrg.*, ASCE, 114(8), 1804–1826.

Mander, J. B., Priestley, M. J. N., and Park, R. (1988b). ''Observed stress-strain behavior of confined concrete.'' *J. Struct. Div.*, ASCE, 114(8), 1827–1849.

Mau, S. T. (1990). ''Effect of tie spacing on inelastic buckling of longitudinal bars.'' *ACI Struct. J.*, 87(6), 671–677.

Mau, S. T., and El-Mabsout, M. (1989). ''Inelastic buckling of reinforcing bars.'' *J. Engrg. Mech.*, ASCE, 115(1), 1–17.

Monti, G., and Nuti, C. (1992). ''Nonlinear cyclic behavior of reinforcing bars including buckling.'' *J. Struct. Engrg.*, ASCE, 118(12), 3268–3284.

Papia, M., and Russo, G. (1989). ''Compressive concrete strain at Buckling of longitudinal reinforcement.'' *J. Struct. Engrg.*, ASCE, 115(2), 382–397.

Papia, M., Russo, G., and Zingone, G. (1988). ''Instability of longitudinal bars in RC columns.'' *J. Struct. Engrg.*, ASCE, 114(2), 445–461.

Russo, G. (1988). ''A buckling model for reinforcing bars.'' *Int. J. Mech. Sci.*, 30(1), 3–11.

Scribner, C. F. (1986). ''Reinforcement buckling in reinforced concrete flexural members.'' *ACI J.*, 83(6), 966–973.

Sheikh, S. A. (1978). ''Effectiveness of rectangular ties as confinement steel in reinforced concrete columns.'' PhD thesis, University of Toronto, Toronto.

Sheikh, S. A., and Khoury, S. S. (1993). ''Confined concrete columns with stubs.'' *ACI Struct. J.*, 90(4), 414–431.

Sheikh, S. A., Shah, D. V., and Khoury, S. S. (1994). ''Confinement of high-strength concrete columns.'' *ACI Struct. J.*, 91(1), 100–111.

Sheikh, S. A., and Uzumeri, S. M. (1982). ''Analytical model for concrete confinement in tied columns.'' *J. Struct. Div.*, ASCE, 108(12), 2703–2722.